Electrical Power and Energy Systems 64 (2015) 626–634

Contents lists available at ScienceDirect

Electrical Power and Energy Systems

journal homepage: www.elsevier.com/locate/ijepes

Robust non-fragile power system stabilizer

M. Soliman *

Electrical Power and Machines Department, Benha University, Cairo, Egypt

ARTICLE INFO

Article history:
Received 16 August 2013
Received in revised form 30 June 2014
Accepted 17 July 2014

Keywords:
Dynamic stability
PSS design
Robustness
Resilient controllers
Kharitonov polynomials

ABSTRACT

This paper presents a step towards the design of robust non-fragile power system stabilizers (PSSs) for single-machine infinite-bus systems. To ensure resiliency of a robust PSS, the proposed approach presents a characterization of all stabilizers that can guarantee robust stability (RS) over wide range of operating conditions. A three-term controller $(x_1 + x_2 s)/(1 + x_3 s)$ is considered to accomplish the design. Necessary and sufficient stability constraints for existing of such controller at certain operating point are derived via Routh–Hurwitz criterion. Continuous variation in the operating point is tackled by an interval plant model where RS problem is reduced to simultaneous stabilization of finite number of plants according to Kharitonov theorem. Controller triplets that can robustly stabilize vertex plants are characterized in a similar manner. The most resilient controller is computed at the center of maximum-area inscribed rectangle. Simulation results confirm robustness and resiliency of the proposed stabilizer.

Introduction

Power system stabilizers (PSSs) are often used to provide supplementary feedback stabilizing signals through the excitation systems. Therefore, the stability limit of power systems can be extended by PSSs which can enhance system damping at low frequency oscillations associated with electromechanical modes [1,2]. The conventional PSS commonly used in practice is a dynamic output feedback, a lead controller type, with a single or double stage and uses the speed deviation $\Delta\omega$ as a feedback signal [3]. Conventional fixed-parameter PSS may fail to maintain system stability over wide range of operating conditions or at least leads to a degraded performance once the deviation from the nominal point becomes significant. Consequently, design of robust PSSs becomes a priority to cope with uncertainties imposed by continuous variation in operating points. Synthesis of robust PSSs has been one of the most celebrated research areas in power system control. Over the past three decades or so, several methods have been developed that enable a PSS to cope with parametric uncertainties in the plant dynamics [4–11]. This is true for both types of uncertainties: structured and unstructured. A common divisor of these methods is that they rely on the celebrated YJBK parameterization [12] of all stabilizing controllers for a fixed linear time-invariant plant, which provides a free parameter over which an appropriate function of a closed-loop transfer function may be minimized. Elegant techniques for minimizing H_∞, H_2 and L_1 norms of different closed loop transfer functions have been developed using this parameterization [4,5]. Moreover, efficient numerical approaches have been subsequently developed [10,11]. Although these methods cope with uncertainty in the plant dynamics, they all assume that the derived parameters of a PSS are precise and exactly implemented. In practice it turns out, however that these gains cannot be implemented exactly (due to resistors' tolerance used with operational amplifiers implemented for continuous-time PSS) leading to fragility problem [13,14]. This raises an important issue that is a robust PSS can be very sensitive, or fragile, with respect to errors or perturbations in the controller coefficients and thus system instability may occur. In turn, that brings about a fundamental problem in robust control system design, which has been recently termed the fragility problem, and hence the design of non-fragile controller opens up as an important research topic that deserves further investigations. Continuous-time PSS implementation uses operational amplifiers with resistors having tolerances in the range of ±5% to ±20%. For discrete-time PSS implementation, imprecision is also expected in analog–digital and digital–analog conversion circuits. Consequently, PSS design has to be able to tolerate some uncertainty in the controller parameters as well as the plant dynamics. Fragility problem of a robust PSS in power system literature is a new topic except for [15]. Static output feedback design that permits for controller perturbation is suggested in [15] where speed deviation ($\Delta\omega$) and rotor angle deviation ($\Delta\delta$) are used for

* Address: Electrical Power and Machines Department, Faculty of Engineering, Benha University, 108 Shoubra St., P.O. Box: 11241, Cairo, Egypt. Tel.: +20 (10) 05419184; fax: +20 (2) 22022310.
E-mail address: msoliman_28@yahoo.com

http://dx.doi.org/10.1016/j.ijepes.2014.07.054
0142-0615/

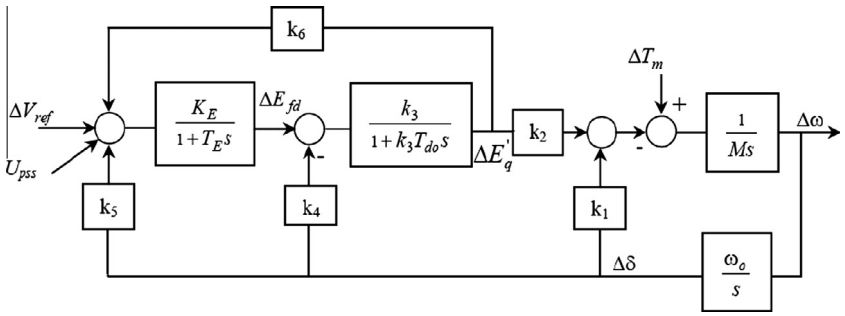

Fig. 1. Block diagram of the linearized model [1].

static feedback and two feedback gains have been computed. The feedback gain of $\Delta\omega$ can allow for a perturbation of +7.2% of its nominal values while that ($\Delta\delta$) has to be implemented exactly.

In this paper, the design of a robust and non-fragile PSS is presented to cope with uncertainties in power system dynamics and tolerate the perturbations in the PSS itself. To realize a robust first order PSS, necessary and sufficient stability conditions are derived using Routh–Hurwitz (RH) criterion. The stability boundaries derived by RH criterion are then plotted in the controller parameter-plane ($x_1 - x_2$) with fixed x_3 where the stability region is examined. Thereafter, the PSS pole time constant is allowed to vary over the typical range considered in PSS industry. The intersection of stability regions at different operating points with $x_3 = [x_3^-\quad x_3^+]$ can help characterize all stabilizing controllers, if it exists. Eight Kharitonov vertex plants are computed for an interval plant model considered to capture all uncertainties in operating point. Thus, the aforementioned approach can be applied only eight times where intersection of stability regions can easily be examined. Such graphical representation of the controller solution set can help select a point in the set such that its minimum distance to the region boundary is maximized, i.e. the center of the maximum-area inscribed rectangular.

The paper is organized as follows. Section 'Problem statement' describes the uncertainties of a simple power system. In Section 'Robust versus non-fragile: overview', an overview of robust and non-fragile control is presented. Necessary and sufficient constraints for characterizing all robust stabilizing PSSs are derived in Section 'Robust PSS design'. Selection of the most resilient PSS is reported in Section 'Non-fragility analysis'. Simulation results are considered in Section 'Simulation results'. Finally, Section 'Conclusion' concludes the paper.

Problem statement

The test system comprises a single-machine connected to an infinite-system through a tie lie line. Such infinite system may represent The venin's equivalent of a large interconnected power system. System dynamics are represented by four non-linear differential equations as given in [8]. Nonlinear model and data of the system are given in the Appendix A where the symbols are standard and have their usual meaning as given in [1]. The block diagram for linearized model of such system as proposed by deMello and Concordia [1] is shown in Fig. 1. The model parameters ($k_1, \ldots, k_6$) are load-dependent and have to be computed at each operating point given by active and reactive powers P, Q.

These parameters can be expressed as explicit functions in P and Q as derived in [8]. Open loop transfer function (TF) is in turn load-dependent and hence it is more convenient to accomplish the design. At any operating point, such TF has a general form given by:

$$G_p(s) = \frac{\Delta\omega}{\Delta U} = \frac{-b_1 s}{a_4 s^4 + a_3 s^3 + a_2 s^2 + a_1 s + a_0} \tag{1}$$

The coefficients a_0, a_1, a_2 and b_1 vary according to a vector ρ which consists of two independent quantities P and Q, i.e., $\rho = [P \quad Q]$ while a_3 and a_4 are always constant and independent of machine loading. Simply, any change in P, Q leads to corresponding changes in a_0, a_1, a_2 and b_1. Therefore, if P and Q vary over their prescribed intervals, i.e. $P \in [P^- \quad P^+]$ and $Q \in [Q^- \quad Q^+]$, Eq. (1) describes a family of plants rather than a nominal plant. Since a_0, a_1, a_2 and b_1 depend simultaneously on ρ, this family of plants can be approximated by an interval plant where:

$$a_4 = [\underline{a}_4 \quad \bar{a}_4], a_3 = [\underline{a}_3 \quad \bar{a}_3], a_2 = [\underline{a}_2 \quad \bar{a}_2], a_1 = [\underline{a}_1 \quad \bar{a}_1],$$
$$a_0 = [\underline{a}_0 \quad \bar{a}_0], b_1 = [\underline{b}_1 \quad \bar{b}_1] \tag{2}$$

where

$$[\underline{a}_i \quad \bar{a}_i] = [\min_{\substack{P\in[\underline{P}\ \bar{P}],\\ Q\in[\underline{Q}\ \bar{Q}]}} a_i / \max_{\substack{P\in[\underline{P}\ \bar{P}],\\ Q\in[\underline{Q}\ \bar{Q}]}} a_i], i = 0, 1, \ldots, 4$$

Robust stability of this interval plant implies that of the family of plants. However, instability of such interval plant does not imply instability of such family of plants. Stability of interval plants is often studied via Kharitonov theorem [12,16].

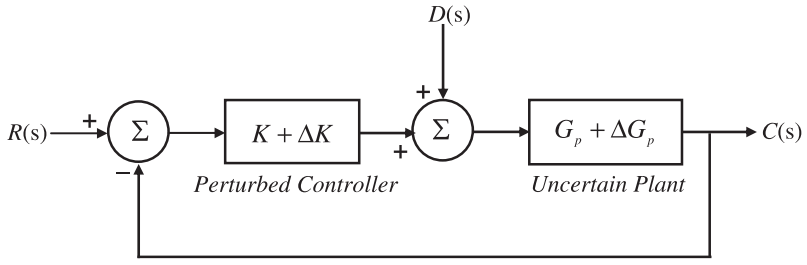

Fig. 2. Uncertain plant with perturbed controller.

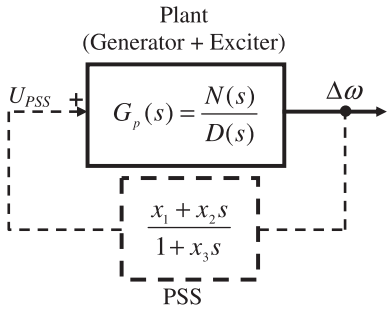

Fig. 3. Test system with a stabilizing three-term PSS.

Robust versus non-fragile: overview

Robust control problem

The robust design problem is often stated as "given a linear plant G_p with additive uncertainties ΔG_p, it is required to find a controller K which internally stabilizes the family of plants $G_p + \Delta G_p$ and satisfies a given performance measure [14]". There are different algorithms that provide an answer to this problem [12–15]. Frequently, the focus is on structured uncertainties in the plant to represent the effect of general time-varying parameters whose exact values are unknown but which are known to belong to a given set. In general, the available algorithms do not incorporate the problems associated with the implementation of uncertain controllers.

Non-fragile control problem

Fragility problem discloses the issue of accuracy of controller implementation to the extent that it brings about a trade-off between implementation accuracy and performance deterioration. It is therefore crucial to address and understand all the effects of controller uncertainties in the implementation of robust controllers, which optimize a prescribed performance measure in linear dynamical systems. It is quite reasonable for various practical purposes to restrict attention to structured uncertainties in the controllers. Therefore, a more realistic robustness problem would be the one incorporating both plant uncertainties and PSS uncertainties as illustrated in Fig. 2.

It has been suggested in [13,14] to overcome the fragility problem to develop synthesis methods which incorporates some structured uncertainties in the controller and then search for the "best" solution guaranteeing a compromise between optimality and fragility; or employ a useful parameterization of the controller.

Robust PSS design

Necessary and sufficient stability constraints

Consider the feedback control system shown in Fig. 3; it has a characteristic polynomial given by:

$$(x_3 s + 1)D(s) + (x_2 s + x_1)N(s) = 0 \tag{3}$$

where $D(s) = (a_4 s^4 + a_3 s^3 + a_2 s^2 + a_1 s + a_0)$, $N(s) = b_1 s$.

Putting $c_5 = x_3 a_4/b_1$, $c_4 = (a_4 + x_3 a_3)/b_1$, $c_3 = (a_3 + x_3 a_3)/b_1$, $c_2 = (a_2 + x_3 a_2)/b_1$, $c_1 = (a_1 + x_3 a_0)/b_1$, and $c_0 = a_0/b_1$, (4) can be rewritten as follows:

$$c_5 s^5 + c_4 s^4 + c_3 s^3 + (c_2 + x_2)s^2 + (c_1 + x_1)s + c_0 = 0 \tag{4}$$

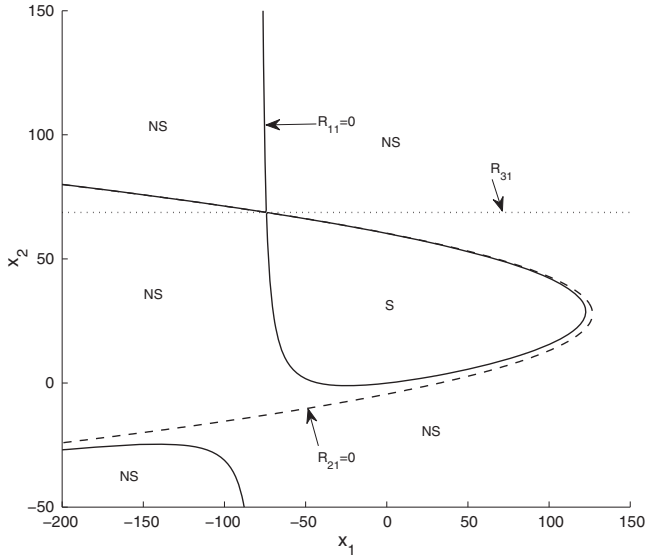

Fig. 4. Stability boundaries of test point at $P = 0.9$, $Q = 0.2$ and $x_3 = 0.085$.

Now, the celebrated Routh–Hurwitz criterion is utilized to derive the set of necessary and sufficient stability constraints as follows:

$$\begin{array}{l|ll} s^5 & c_5 & c_3 & c_1 + x_1 \\ s^4 & c_4 & c_2 + x_2 & c_0 \\ s^3 & R_{31} & c_4(c_1 + x_1) - c_0 c_5 \\ s^2 & R_{21} & c_0(c_3 c_4 - c_5(c_2 + x_2)) \\ s^1 & R_{11} \\ s^0 & R_{01} \end{array}$$

where

$$R_{31} = c_3 c_4 - (c_2 + x_2)c_5,$$

$$R_{21} = c_3 c_4 (c_2 + x_2) - c_5 (c_2 + x_2)^2 - c_4^2 (c_1 + x_1) + c_0 c_4 c_5$$

$$R_{11} = \{c_3 c_4 (c_2 + x_2) - c_5 (c_2 + x_2)^2 - c_4^2 (c_1 + x_1) + c_0 c_4 c_5\} \times \{c_4 (c_1 + x_1) - c_0 c_5\} - c_0 (c_3 c_4 - c_5 (c_2 + x_2))^2$$

$$R_{01} = c_0 (c_3 c_4 - c_5 (c_2 + x_2))$$

Stability constraints are simply written as follows: $R_{i1} > 0$, $i = 0, 1, 2, 3$ where stability boundaries are given by zero-equalities, i.e. $R_{i1} = 0$, $i = 0, 1, 2, 3$. The positivity of R_{31} is ensured *iff* $x_2 < (c_3 c_4 - c_2 c_5)/c_5$ which in turn makes $R_{01} > 0$ feasible. A test point at $P = 0.9$ pu, $Q = 0.2$ pu and $x_3 = 0.85$ s is considered to illustrate the stability boundaries as shown in Fig. 4. Testing a few points in the controller parameter-plane, as shown in Fig. 4, can help identify the stability region where "NS" stands for "*Unstable*" and "S" stands for "*Stable*". It can be noticed that stability region is completely bounded by the constraint $R_{11} = 0$ (solid line) which is a subset of that bounded by $R_{21} = 0$ (dashed-line). A typical range of a PSS pole time-constant is frequently given by $x_3 = [0.02 \quad 0.15]$ as explained in [2]. Typically, PSS design is often carried out at some values in this interval [8,10,11].

Hint: Matlab function "ezplot" can help plotting stability constraints. The syntax "ezplot (f, [xmin, xmax, ymin, ymax])" plots $f(x, y) = 0$ over $x_{\min} < x < x_{\max}$ and $y_{\min} < y < y_{\max}$.

The stability region can explicitly be determined by the following simple mathematical manipulations. The condition $R_{11} = 0$ can be formulated as follows:

$$\alpha x_2^2 + \lambda x_2 + \gamma = 0$$

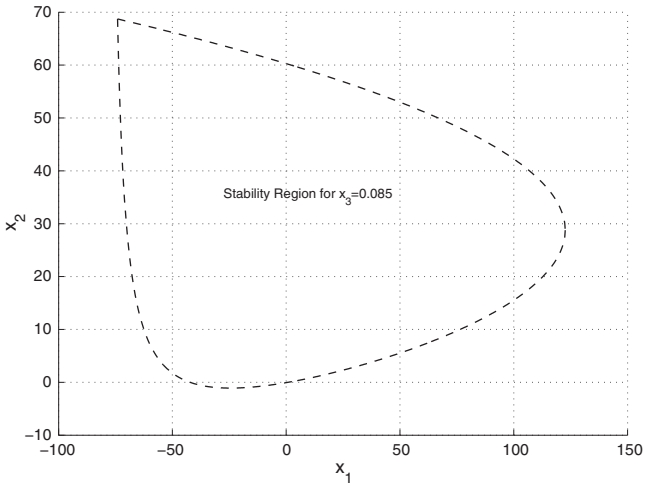

Fig. 5. Stability region of a test point at $P = 0.9$, $Q = 0.2$ and $x_3 = 0.085$.

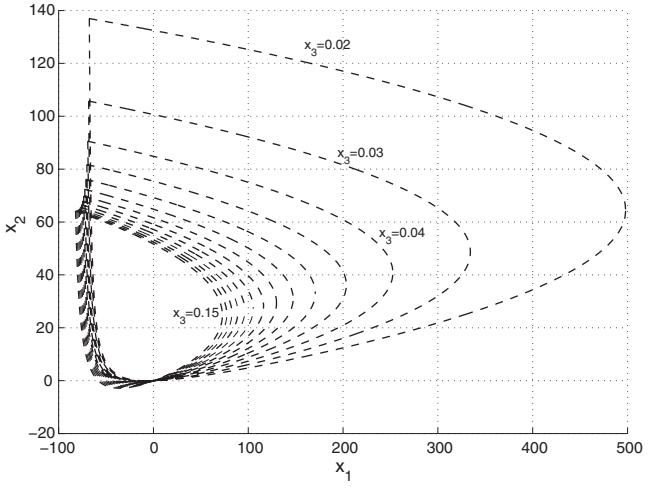

Fig. 6. Stability region of a test point at $P = 0.9$, $Q = 0.2$ and $x_3 = [0.02\ 0.15]$.

where $\alpha = \alpha_0 + \alpha_1 x_1$, $\alpha_0 = -c_1c_4c_5$, $\alpha_1 = -c_4c_5$

$$\lambda = \lambda_0 + \lambda_1 x_1, \lambda_0 = c_1c_3c_4^2 - 2c_1c_2c_4c_5 + c_0c_3c_4c_5, \lambda_1 = c_3c_4^2 - 2c_2c_4c_5$$

$$\gamma = \gamma_0 + \gamma_1 x_1 + \gamma_2 x_1^2, \gamma_0 = c_0c_2c_3c_4c_5 - c_1c_2^2c_4c_5 + c_1c_2c_3c_4^2 + 2c_0c_1c_4^2c_5 - c_0^2c_4c_5^2 - c_0c_3^2c_4^2 - c_1^2c_4^3$$

$$\gamma_1 = c_2c_3c_4^2 - c_2^2c_4c_5 - 2c_1c_4^3 + 2c_0c_4^2c_5, \gamma_2 = -c_4^3$$

Quadratic equation characterizer results in a 3rd order equation in x_1 as follows:

$$\lambda^2 - 4\alpha\gamma = \phi_3 x_1^3 + \phi_2 x_1^2 + \phi_1 x_1 + \phi_0, \phi_3 = -4\alpha_1\gamma_2, \phi_2 = \lambda_1^2 - 4(\alpha_0\gamma_2 + \alpha_1\gamma_1),$$
$$\phi_1 = 2\lambda_0\lambda_1 - 4(\gamma_0\alpha_1 - \gamma_1\alpha_0), \phi_0 = \lambda_0^2 - 4\alpha_0\gamma_0$$

The roots of such equation determine the extreme points of x_1 that realize real and equal roots of x_2. The stability region shown in Fig. 4 is explicitly illustrated in Fig. 5. The effect of variation of the controller-pole time constant on the stability region is shown in Fig. 6 using a step size of 0.01. The coefficients of the open loop transfer function are continuous over the ranges of P and Q such that each point has a steadily load flow solution. As a result, these ranges are mapped into controller parameters-plane of $x_1 - x_2$ at

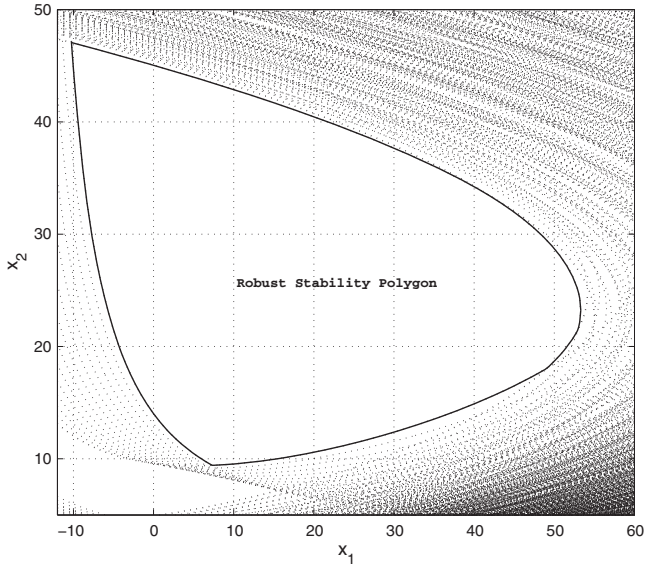

Fig. 7. Stability regions for $P = [0.21.0]$, $Q = [-0.20.5]$ and $x_3 = [0.020.15]$.

fixed x_3. Two approaches are proposed to study the effect of variation of P and Q on the resultant stability region while x_3 belongs to $x_3 = [x_3^- x_3^+]$. The first approach utilizes image-set polynomials while the second utilizes Kharitonov polynomials. The number of polynomials in the first approach depends mainly on the step size selected to scan the intervals of P and Q, while the second approach utilizes only eight polynomials according to Kharitonov theorem.

Image-set polynomials

The stability regions of different plants in the operating range of P and Q can be plotted using an appropriate step size. The choice of the step size is arbitrary and it is chosen to produce clearly defined stability boundaries. Further, the controller-pole time constant is allowed to vary over its interval. Now the following ranges $P = [0.2\quad 1.0]$, $Q = [-0.2\quad 0.5]$ and $x_3 = [0.02\quad 0.15]$ are

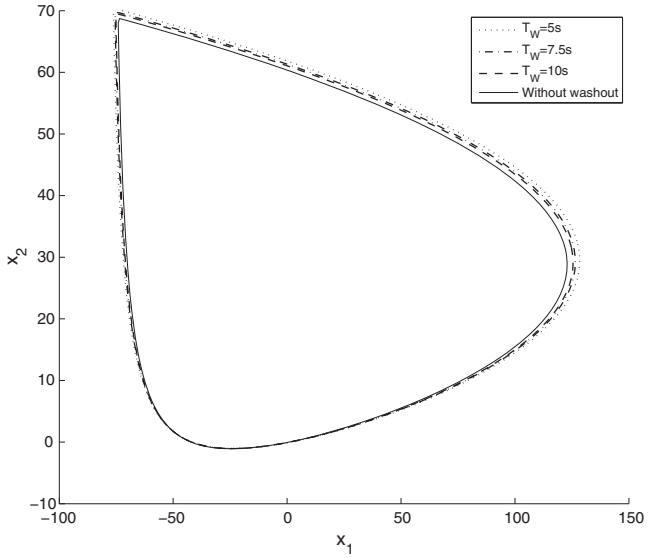

Fig. 8. Effect of T_W on the stability region of a test point given by $P = 0.9$ pu, $Q = 0.2$ pu and $x_3 = 0.085$.

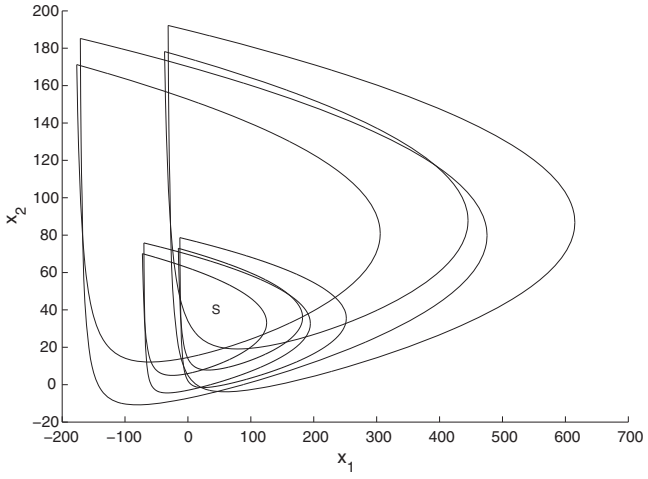

Fig. 9. Stability regions for Kharitonov plants: $x_3 = 0.05$.

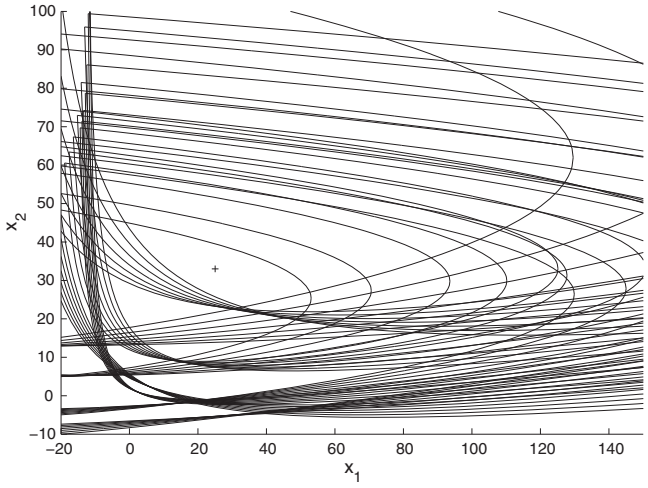

Fig. 10. Stability region for Kharitonov plants with $x_3 = [0.02\ 0.08]$.

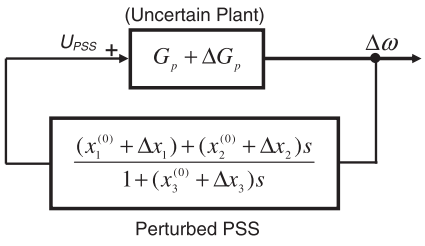

Fig. 11. Uncertain system with Perturbed PSS.

considered. A step size of 0.05 is considered for *P*, Q, and 0.01 for x_3. The stability regions of these ranges are illustrated in Fig. 7. The intersection of these regions characterizes the set of all stabilizing controllers that guarantee robust stability over these ranges.

Remark 1. Using image-set polynomials results in accurate stability region in the controller-parameter plane, however it require plotting the stability boundaries of 3570 plants that cover the full ranges of *P*, *Q* and x_3 with the specified step size, i.e. increasing computational effort.

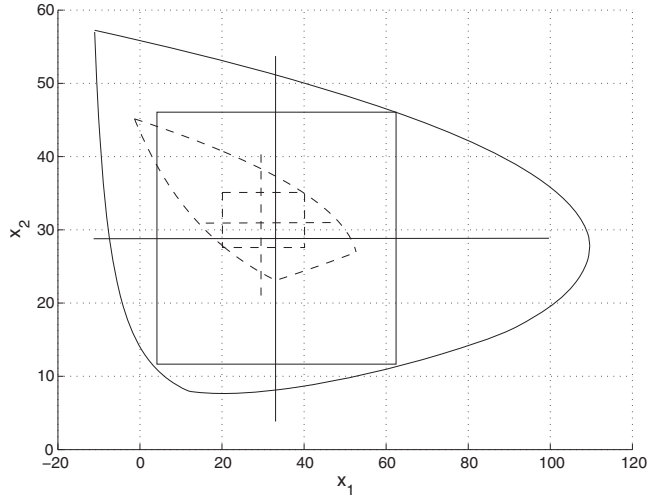

Fig. 12. Maximum-area inscribed rectangular with $x_3 = [0.02\ 0.08]$: Image-set polynomials (*solid line*) versus Kharitonov polynomials (*dashed line*).

Remark 2. Although a digital PSS is quite precise, still it has uncertainties such as finite word length, imprecision in analogue to digital and digital to analogue conversion circuits, finite resolution measurements and round-off errors in numerical computations. Hence, discrete time PSS may be fragile if these uncertainties are not considered.

A typical PSS model has three basic blocks: the gain, the washout filter, and the phase-lead compensator, as given below:

$$G_{pss}(s) = K\frac{T_W s}{1+T_W s}\frac{1+T_1 s}{1+T_2 s} = G_W(s)\frac{K+KT_1 s}{1+T_2 s} = G_W(s)\left(\frac{x_1+x_2 s}{1+x_3 s}\right)$$

The purpose of the washout filter is to ensure that there is no steady state error of voltage reference due speed deviation [2]. The PSS should be activated only when low frequency oscillations develop, and should be automatically terminated when these oscillations ceases. It should not interfere with the regular function of the excitation system during steady state operation of the system frequency. Since the washout filter should not have any effect on the phase shift or gain at the oscillating frequency, it can be achieved by choosing a large value of T_W so that sT_W is much larger

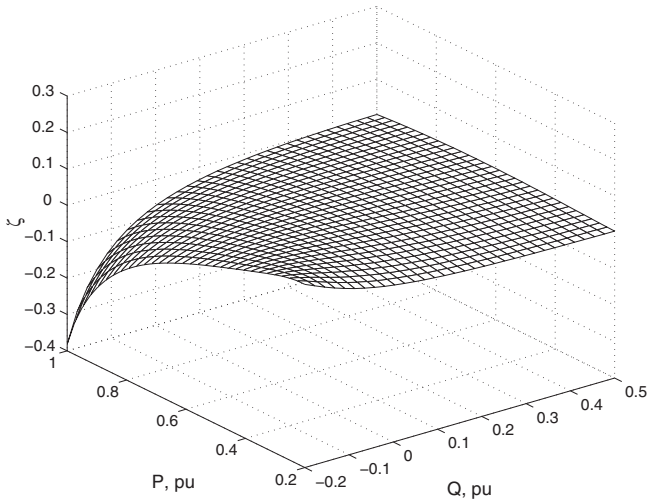

Fig. 13. Damping ratios of the dominant open loop poles of 1024 points.

than unity and hence $G_W(j\omega_n) \approx 1$, where ω_n is the oscillating frequency. Further, its phase contribution is close to zero. The PSS will not have effect on the steady state of the system since, in steady state, $\Delta\omega = 0$. The impact of including the washout filter in the design approach is shown in Fig. 8 considering different values of T_W. Remarkably, its effect on the stability region is not significant.

Kharitonov polynomials

Based on the interval plant model (3), only eight vertex plants have to be considered to guarantee robustness under load uncertainties. Necessary and sufficient conditions for robust stability of interval plants according to Kharitonov theorem can be found in [12].

Definition 1. Consider the set f of all real polynomials of degree n of the from $p(s) = a_0 + a_1 s + a_2 s_2 + \ldots + a_n s^n$, where the coefficients vary over independent intervals i.e. $a_0 = [\underline{a}_0 \quad \bar{a}_0], a_1 = [\underline{a}_1 \quad \bar{a}_1], \ldots, a_n = [\underline{a}_n \quad \bar{a}_n]$. Such a set of polynomials is called an interval polynomial.

Theorem 1. [12] *Every polynomial in the interval family f is Hurwitz-stable iff the following Kharitonov polynomials are Hurwitz-stable*:

$$K^1(s) = \underline{a}_0 + \underline{a}_1 s + \bar{a}_2 s^2 + \bar{a}_3 s^3 + \underline{a}_4 s^4 + \underline{a}_5 s^5 + \bar{a}_6 s^6 + \ldots$$

$$K^2(s) = \underline{a}_0 + \bar{a}_1 s + \bar{a}_2 s^2 + \underline{a}_3 s^3 + \underline{a}_4 s^4 + \bar{a}_5 s^5 + \bar{a}_6 s^6 + \ldots$$

$$K^3(s) = \bar{a}_0 + \underline{a}_1 s + \underline{a}_2 s^2 + \bar{a}_3 s^3 + \bar{a}_4 s^4 + \underline{a}_5 s^5 + \underline{a}_6 s^6 + \ldots$$

$$K^4(s) = \bar{a}_0 + \bar{a}_1 s + \underline{a}_2 s^2 + \underline{a}_3 s^3 + \bar{a}_4 s^4 + \bar{a}_5 s^5 + \underline{a}_6 s^6 + \ldots$$

Proof. See [12]. □

Applying this theorem to system (1) whose parameters are given by (3), the controller has to simultaneously stabilize the following vertex plants:

$$(x_3 s + 1)D_i(s) + (x_2 s + x_1)N_j(s) = 0, \quad i = 1,2,3,4, \quad j = 1,2$$

Eight vertex polynomials are termed as $\Delta_i, i = 1, 2, \ldots, 8$ and given as follows:

$$\Delta_1 = (x_3 s + 1)(\underline{a}_4 s^4 + \bar{a}_3 s^3 + \bar{a}_2 s^2 + \underline{a}_1 s + \underline{a}_0) + (x_2 s + x_1)(\underline{b}_1 s)$$

$$\Delta_2 = (x_3 s + 1)(\underline{a}_4 s^4 + \underline{a}_3 s^3 + \bar{a}_2 s^2 + \bar{a}_1 s + \underline{a}_0) + (x_2 s + x_1)(\underline{b}_1 s)$$

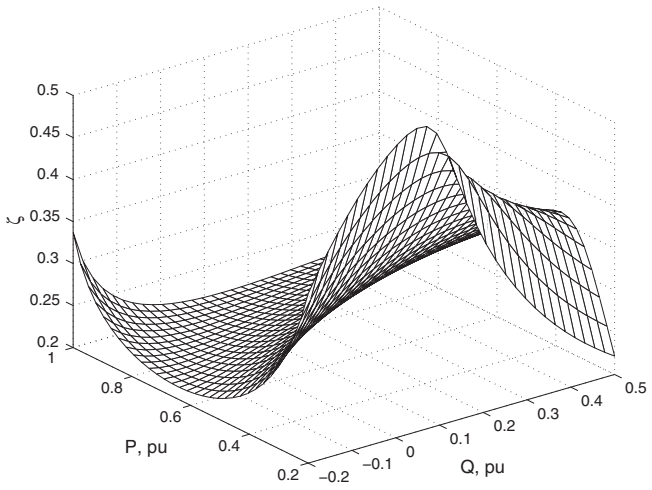

Fig. 14. Damping ratios of the dominant closed loop poles of 1024 plants with exact controller gains.

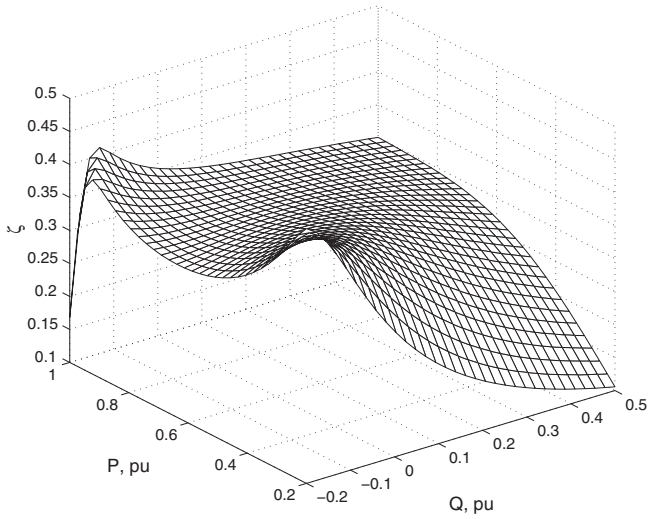

Fig. 15. Damping ratios of the dominant closed loop poles of 1024 plants with perturbed controller gains (−30%).

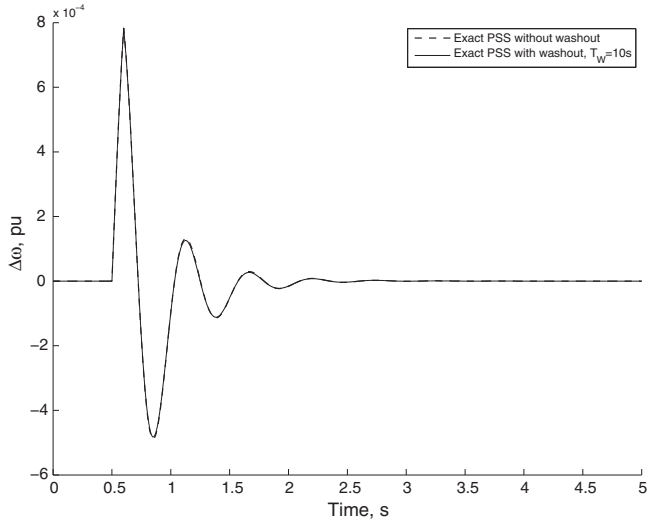

Fig. 16. Speed deviation response for 0.1 pu increment in T_m with and without washout filter.

$$\Delta_3 = (x_3 s + 1)(\bar{a}_4 s^4 + \bar{a}_3 s^3 + \underline{a}_2 s^2 + \underline{a}_1 s + \bar{a}_0) + (x_2 s + x_1)(\underline{b}_1 s)$$

$$\Delta_4 = (x_3 s + 1)(\bar{a}_4 s^4 + \underline{a}_3 s^3 + \underline{a}_2 s^2 + \bar{a}_1 s + \bar{a}_0) + (x_2 s + x_1)(\underline{b}_1 s)$$

$$\Delta_5 = (x_3 s + 1)(\underline{a}_4 s^4 + \bar{a}_3 s^3 + \bar{a}_2 s^2 + \underline{a}_1 s + \underline{a}_0) + (x_2 s + x_1)(\bar{b}_1 s)$$

$$\Delta_6 = (x_3 s + 1)(\underline{a}_4 s^4 + \underline{a}_3 s^3 + \bar{a}_2 s^2 + \bar{a}_1 s + \underline{a}_0) + (x_2 s + x_1)(\bar{b}_1 s)$$

$$\Delta_7 = (x_3 s + 1)(\bar{a}_4 s^4 + \bar{a}_3 s^3 + \underline{a}_2 s^2 + \underline{a}_1 s + \bar{a}_0) + (x_2 s + x_1)(\bar{b}_1 s)$$

$$\Delta_8 = (x_3 s + 1)(\bar{a}_4 s^4 + \underline{a}_3 s^3 + \underline{a}_2 s^2 + \bar{a}_1 s + \bar{a}_0) + (x_2 s + x_1)(\bar{b}_1 s)$$

The bounds of each coefficient are computed for the prescribed ranges of P and Q and given by: $a_4 = [1 \quad 1]$, $a_3 = [20.46 \quad 20.46]$, $a_2 = [22.41 \quad 87.21]$, $a_1 = [131.5 \quad 793]$, $a_0 = [707.4 \quad 1763.7]$, $b_1 = [2.44 \quad 11.57]$ Accordingly, the stability regions of the above eight polynomials at $x_3 = 0.05$ are shown in Fig. 9. Stability constraints do not tolerate for $x_3 = [0.020.15]$, i.e. no intersection occurs. A reasonable suggestion is to reduce the upper bound of x_3 gradually until a feasible solution **"polygon"** is obtained. A

reduced range of $x_3 = [0.02 \quad 0.08]$ can result in a solution set as shown in Fig. 10.

Non-fragility analysis

To enhance non-fragility of a robust power system stabilizer shown in Fig. 11, robust stability basin is searched for the point $(x_1^{(0)}, x_2^{(0)}, x_3^{(0)})$ that allows for maximum perturbations in the controller parameters $(\Delta x_1, \Delta x_2, \Delta x_3)$. Characterization of all robust controllers is firstly developed where convex polygon shown in Fig. 7 characterizes all robust stabilizing PSSs considering the full range of the controller-pole time constant, i.e. $x_3 = [0.02 \quad 0.15]$ using image-set polynomials, while the convex polygon shown in Fig. 10 characterizes all stabilizing PSSs for $x_3 = [0.02 \quad 0.08]$ using Kharitonov polynomials.

In this paper, the most non-fragile PSS is selected at the center of the maximum-area inscribed rectangle that permits for maximum dependent variations in the parameters of the controller. For fair comparison between image-set polynomials and Kharitonov polynomials, the study is carried out for the reduced range of x_3. It is clear from Fig. 12 that the stability region by Kharitonov is a subset of that obtained by image-set polynomials, and therefore the maximum-area inscribed rectangle of the latter is larger than that of the first. Hereafter, the maximum allowable ranges for x_1 and x_2 while $x_3 = [0.02 \quad 0.08]$ are given by $x_1 \cong [4 \quad 62]$, $x_2 \cong [11 \quad 47]$ for image-set polynomials and given by $x_1 \cong [20 \quad 40]$, $x_2 \cong [27 \quad 35]$ for Kharitonov polynomials. The most-resilient controller is considered at the center of the box of controller parameters as follows:

Image-set polynomials: $x_1^{(0)} = 33, x_2^{(0)} = 19, x_3^{(0)} = 0.05$

Kharitonov polynomials: $x_1^{(0)} = 30, x_2^{(0)} = 31, x_3^{(0)} = 0.05$

These values permit for maximum allowable controller perturbations.

Simulation results

Single-machine infinite-bus system

Open loop response

The roots of the open-loop system are calculated for 1024 points in the full range of P and Q. Fig. 13 illustrates the dominant roots. Remarkably, the system achieves negative damping at certain operating points.

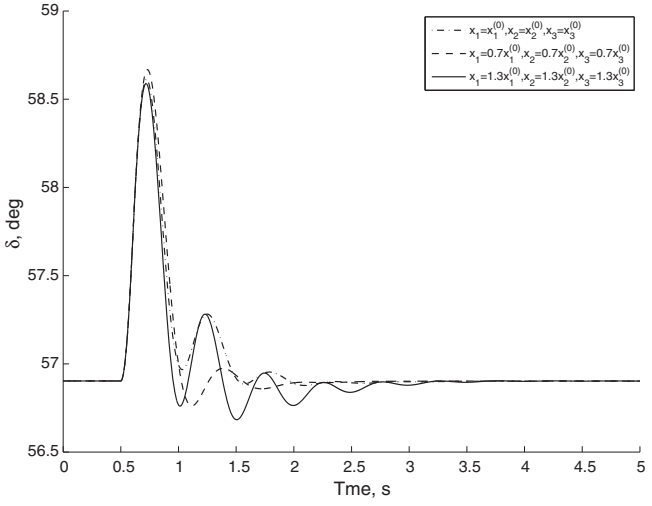

Fig. 17. Rotor angle response for 0.1 pu increment in T_m with exact and perturbed PSSs.

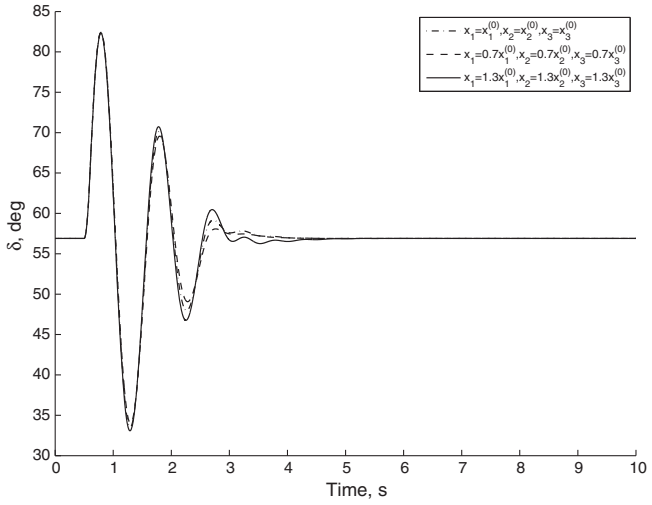

Fig. 18. Rotor angle response for 3-phase short circuit at the infinite bus for 100 ms with exact and perturbed PSSs.

Robust stability of exact controller $\{x_1^{(0)}, x_2^{(0)}, x_3^{(0)}\}$.

The most resilient controller is selected as $x_1 = 33$, $x_2 = 19$, $x_3 = 0.05$. The effectiveness of such controller, to guarantee robust stability over the entire range of P and Q is depicted in Fig. 14. The dominant roots of the characteristic polynomial dominant roots for a fine grid covering the whole operating range are illustrated. Remarkably, the minimum damping ratio greater than 0.2 is achieved for the entire family of plants.

Robust stability of −30% perturbed controller

The gains of the exact controller are all reduced by 30%, i.e. $x_1 = 0.7x_1^{(0)}, x_3 = 0.7x_2^{(0)}, x_3 = 0.7x_3^{(0)}$. The effectiveness of the perturbed controller, to guarantee robust stability over the entire range of P and Q, is depicted in Fig. 15 where a minimum damping ratio of 0.2 is achieved.

Nonlinear model simulation

Using the nonlinear model of the SMIB system given in the Appendix A, the resilient PSS is simulated at an operating point given by $P = 0.9$ pu and $Q = 0.4$ pu. The controller's output is saturated at ±0.1 pu that cannot affect the profile of the terminal voltage dramatically. In this study, mechanical torque disturbance and three-phase short circuit are considered. Firstly, the system

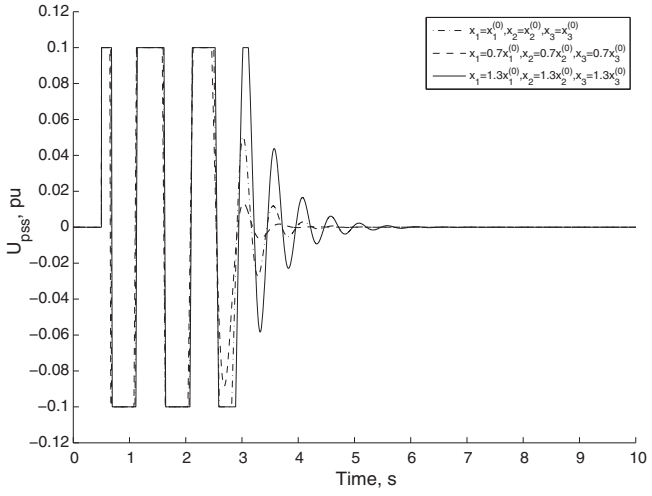

Fig. 19. Feedback stabilizing signals under the three-phase short circuit disturbance with exact and perturbed PSSs.

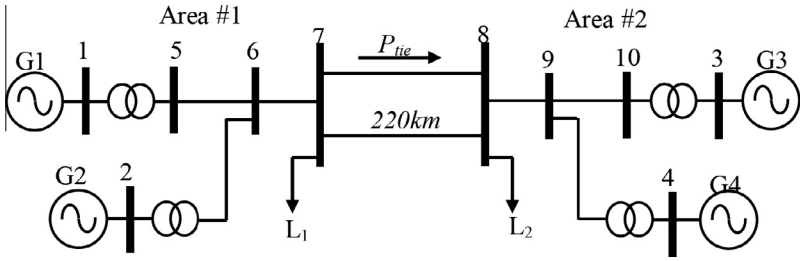

Fig. 20. Two-area four-machine test system [2].

response for 0.1 pu step increment in the mechanical torque with full recovery after 100 ms is depicted in Fig. 16. Remarkably, the proposed PSS can enhance system damping; further, the effect of inclusion of the washout filter on the system response is nearly non-significant. The resiliency of the proposed PSS is examined by considering the rotor angle response for the same disturbance with exact and perturbed controllers as shown in Fig. 17. Furthermore, the performance of the proposed resilient PSS, when the system undergoes three-phase to ground fault at the infinite bus for 100 ms, is shown in Fig. 18. Noticeably, the design is non-fragile even under large disturbances. The feedback stabilizing signals under three-phase short circuit disturbance is shown in Fig. 19.

Multimachine simulation

Multimachine power system is a multi-input multi-output (MIMO) system and hence it violates theoretically the basic requirements of the proposed approach because it is not a SISO system and it has many PSSs that have more than three terms. Consequently, the proposed approach cannot be applied to multimachine systems directly. Firstly, a multimachine system is decomposed into a set of single-machine subsystem using Thevenin's theorem (the classical approach). Each subsystem comprises one machine connected to hypothetical infinite bus through an equivalent tie line. This decomposition enables us to consider the uncertainties in P and Q of each machine separately. This approach neglects the interaction between different control loops since the design is accomplished for each machine separately.

In this study, two-area four-machine test power system [17] shown in Fig. 20 is considered. This system is available as a MATLAB/SIMULINK demo [18]. In addition, it is equipped with well-tuned power system stabilizers including the standard IEEE PSS4B [19] and the conventional PSS [17]. This gives credit to the comparison with the proposed PSS. The loads are represented by constant impedances, and split between the two areas. Therefore, the equivalent single-machine subsystems are roughly identical due system symmetry. Consequently, the design is carried out once for one equivalent subsystem whilst the resulting stabilizer is added to the four machines. The equivalent tie-line reactance for each machine is computed using Thevenin's theorem. It is assumed that the intervals of P and Q at each machine bus are given by $P = [0.4 \quad 1], Q = [0.0 \quad 0.5]$. The design approach presented in Sections 'Robust PSS design and Non-fragility analysis' is utilized to compute the controller stability regions and then the most non-fragile PSS are computed as before. The parameters of the most resilient PSSs are computed roughly at the center of the maximum-area inscribed rectangle as $x_1^{(0)} = 50, x_2^{(0)} = 30, x_3^{(0)} = 0.03$. The robustness and non-fragility of the proposed design are examined under small and large disturbances. Firstly, the system response due to 10% increment in the load of Area 2 with full recovery after nine seconds is shown in Fig. 21. The proposed design outperforms the conventional PSS and the IEEE-PSS4B stabilizer, and can extend the system stability limits. Secondly, the system is tested for a three-phase to ground fault, at 80 km far from Bus 8, and the response is depicted in Fig. 22. Noticeably, the standard IEEE-PSS4B stabilizer and the conventional design failed to maintain system stability while the proposed design preserves the system stability. Although the design is carried out for approximated models derived using Thevenin's theorem, the proposed PSSs can damp out both local and inter-area modes of oscillation, and tolerate with uncertainties in the plant and the controller itself.

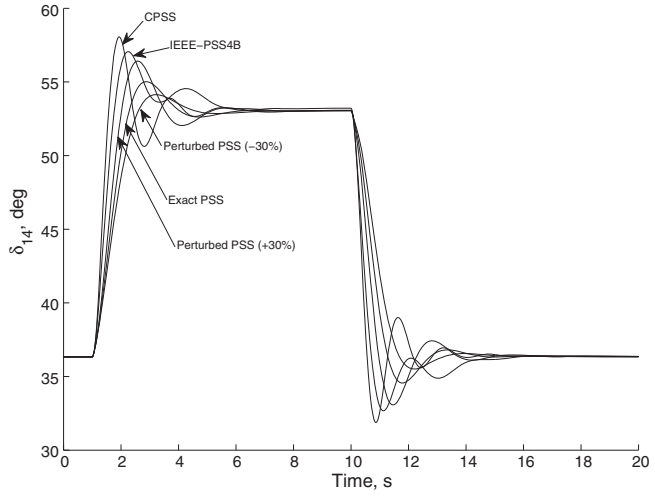

Fig. 21. System response due to 10% increment in the load of Area #2 with full recovery after 9 s.

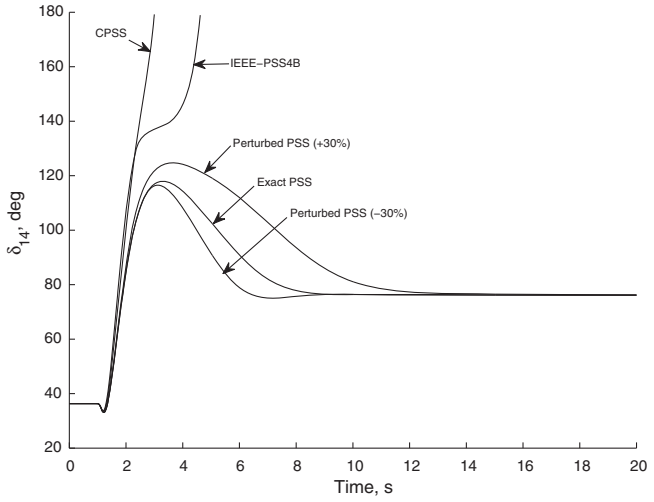

Fig. 22. System response due to three-phase to ground fault on one tie line at 80 km far from Bus #8 for 133 ms.

Conclusion

This paper presents a step towards the design of robust resilient PSSs for single machine infinite-bus systems. A three-term controller is suggested to complete the study. A complete characterization of all PSSs is presented using Routh–Hurwitz criterion to determine necessary and sufficient stability constraints. Such constraints are reformulated to generate the convex stability polygon. Convex polygons are generated for different operating points that cover the operating range and further the typical range of the controller pole. The intersection of such polygons exactly describes the robust stability polygon. To consider finite number of plants, Kharitonov vertices are considered where the former approaches apply. Finally, the most resilient controller is selected at center of the maximum area-inscribed rectangle in the RS polygon to allow for maximum perturbations in the controller parameters. Simulations results based on SMIB and multimachine models are carried out to reveal the effectiveness of the proposed approach.

Appendix A. The nonlinear model

$$\dot{\delta} = \omega_o(\omega - 1)$$
$$\dot{\omega} = (T_m - (E'_q I_q + (X_q - X'_d) I_d I_q))/M$$

$$\dot{E}'_q = -(E'_q + (X_d - X'_d) I_d - E_{fd})/T'_{do}$$
$$\dot{E}_{fd} = (K_E V_{ref} + U_{pss} - K_E V_T - E_{fd})/T_E$$

$$R_e I_d - (X_e + X_q) I_q + V^{\infty} \sin\delta = 0$$
$$R_e I_q + (X_e + X'_d) I_d + E'_q + V^{\infty} \cos\delta = 0$$

Appendix B. Data of a single-machine infinite-bus system

$$X_d = 1.6 \text{ pu}, X_q = 1.55 \text{ pu}, X'_d = 0.32 \text{ pu}, T'_{do} = 6s, M = 10\, s, K_E = 25, T_E = 0.05\, s, E_{fd}^{\min} = -5 \text{ pu}, E_{fd}^{\max} = 5 \text{ pu},$$

$$x_e = 0.4 \text{ pu}, V^{\infty} = 1 \text{ pu}, \omega_o = 2\pi \times 50 \text{ rad/s}.$$

References

[1] DeMello FP, Concordia C. Concepts of synchronous machine stability as affected by excitation control. IEEE Trans Power Appar Syst 1969;88(4):316–29.
[2] Sauer PW, Pai MA. Power system dynamics and stability. Prentice-Hall Inc.; 1998.
[3] Larsen EV, Swann DA. Applying power system stabilizers: Parts I–III. IEEE Trans Power Appar Syst 1981;100(6):3017–46.
[4] Soliman EA, Emara D, Elshafei A, Bhagat A, Malik OP. Robust output feedback power system stabilizer design: an LMI approach. IEEE/PES general meeting; 2008. p. 1–8.
[5] Werner H, Korba P, Chen Yang T. Robust tuning of power system stabilizers using LMI techniques. IEEE Trans Control Syst Technol 2003;11(1):147–2003.
[6] Rao PS, Sen I. Robust pole placement stabilizer design using linear matrix inequalities. IEEE Trans Power Syst 2000;15(1):313–9. February.
[7] Rao PS, Sen I. Robust tuning of power system Stabilizers using QFT. IEEE Trans Control Syst Technol 1999;7(4):478–86.
[8] Soliman HM, Elshafei AL, Shaltout A, Morsi MF. Robust power system stabilizer. IEE Proc Generat, Trans Distribut 2000;147(5):285–91. September.
[9] Djukanovic M, Khammash M, Vittal V. Sensitivity based structured singular value approach to stability robustness of power systems. IEEE Trans Power Syst 2000;15(2):825–30. May.
[10] Abdel-Magid YL, Abido MA. Optimal multiobjective design of robust power system stabilizers using genetic algorithms. IEEE Trans Power Syst 2003;18(3):1125–32. August.
[11] Abido MA. Particle swarm optimization for multimachine power system stabilizer design. IEEE/PES, summer meeting, vol. 3; 15–19 July 2001. p. 1346–51.
[12] Bhattacharyya SP, Chapellat H, Keel LH. Robust control: the parametric approach. Prentice-Hall; 1995.
[13] Keel LH, Bhattacharyya SP. Robust, fragile or optimal. IEEE Trans Automat Contr 1997;42(8):1098–105.
[14] Mahmoud Magdi S. Resilient control of uncertain dynamical systems. Berlin, Heidelberg: Springer-Verlag; 2004.
[15] Soliman HM, Mahmoud MS. Resilient static output feedback power system stabilizer using PSO-LMI optimization. Int J Syst. Contr. Comm 2013;5(1):74–91.
[16] Kharitonov VL. Asymptotic stability of an equilibrium position of a family of systems of linear differential equations. Differential'nye Uravnenya 1978;14(11):2086–8.
[17] Kundur P. Power system stability and control. New York: McGraw-Hill; 1994.
[18] Hydro-Québec, TEQSIM International. Power system blockset for use with Simulink. User's Guide, Natick, MA: The Math Works; 1998.
[19] IEEE Power Engineering Society. IEEE Recommended practice for excitation system models for power system stability studies. IEEE Std 421.5™-2005; 2006.